Phonon densities of states of $La_{2-x}Sr_xNiO_4$: Evidence for strong electron-lattice coupling

R. J. McQueeney and J. L. Sarrao
Los Alamos National Laboratory, Los Alamos, New Mexico 87545

R. Osborn
Argonne National Laboratory, Argonne, Illinois 60439

(Received 22 June 1998)

The inelastic neutron-scattering spectra were measured for several Sr concentrations of polycrystalline $La_{2-x}Sr_xNiO_4$. We find that the generalized phonon density-of-states is the same for $x=0$ and $x=1/8$. For $x=1/3$ and $x=1/2$, the band of phonons corresponding to the in-plane oxygen vibrations (80–90 meV) splits into two subbands centered at 75 and 85 meV. The lower frequency band increases in amplitude for the $x=1/2$ sample, indicating that it is directly related to the hole concentration. These changes are associated with the coupling of oxygen vibrations to doped holes which reside in the NiO_2 planes and are a signature of strong electron-lattice coupling. [S0163-1829(99)02126-8]

Over the past few years, an interesting picture of the $La_{2-x}Sr_xNiO_{4+\delta}$ system has been developing. Interest in this system was resurrected after the discovery of superconductivity in the isostructural hole-doped La_2CuO_4 in hopes that certain compositions of the nickelate would also superconduct. Both undoped materials are antiferromagnetic insulators and holes are doped into the transition-metal-oxide plane via oxygen addition or substitution of a $2+$ ion for La^{3+}. However, the Ni^{2+} $3d^8$ ion is in a high-spin configuration with $S=1$ and the Ni-O charge transfer gap is 4 eV,[1] as opposed to a $S=1/2$ Cu spin with a 2 eV charge gap for the cuprate.[2] This distinction is apparently important, because the addition of a small concentration of holes ($x>0.05$) forms a metallic state and eventually leads to superconductivity in the cuprate, while holes form localized polaronic states in the nickel oxide planes and the compound remains an insulator up to $x=1$.[3] Furthermore, at low temperatures and above $x\approx 0.1$, neutron diffraction,[4,5] electron diffraction,[6] magnetic susceptibility,[7] and various other bulk probes,[8] support a picture that doped holes in the nickelate aggregate to form domain walls (stripes) which separate regions of antiphase antiferromagnetism.[9]

Fundamentally, it is important to determine which interactions are creating the polaronic and ''stripe'' states. Theoretical studies have shown that polaronic and/or stripe states are formed due to the competition between long-ranged Coulomb repulsion of the doped holes and short-ranged attractive interactions such as magnetic confinement effects or electron-lattice coupling.[10–14] It is apparent that Coulomb repulsion and short-ranged magnetic confinement effects alone can create polaronic and striped states;[10,11] however, other theoretical results indicate that electron-lattice coupling can further stabilize the local hole states.[12–15]

The question of the balance of these or other interactions may come into play in order to explain several aspects of recent neutron-diffraction data; in particular, the observation of the occurrence of charge order before magnetic order in the striped phase[4,5] the position of the stripe order in the NiO_2 plane (Ni-centered or O-centered),[16] and the temperature dependence of this position and also of the stripe spacing (incommensurability).[5,16] It has been suggested that competing short-ranged interactions are likely at the root of these questions, and recent theoretical studies have shown that the strength of the electron-lattice coupling can dictate the stripe position.[14]

It is thus very important to measure the strength of the electron-lattice coupling in the nickelates. To date, many experimental studies of the lattice dynamics of the nickelates have demonstrated that strong electron-lattice coupling effects are present. In particular, Raman[17,18] and infrared[19] measurements of zone-center phonons in $La_{5/3}Sr_{1/3}NiO_4$ demonstrate that below the charge-ordering temperature $T_{co}\approx 240$ K, extra modes (or a splitting of modes) are observed which are related to the lower symmetry superlattice structure. At present, the single-crystal phonon dispersion and generalized phonon density of states have been measured by inelastic neutron scattering only for $La_{1.9}NiO_{3.87}$.[20,21] The phonon-dispersion curves in this nonstoichiometric compound show susceptibility to a NiO_2 planar oxygen breathing mode deformability presumably arising from coupling to holes.

Additionally, it is of interest to compare the electron-lattice coupling signatures in the nickelate to those of the cuprate. The cuprates are known to have strong softening of in-plane longitudinal oxygen phonons with the addition of a relatively small concentration of holes (x less than 0.1). Such features are observed in single-crystal measurements of the phonon dispersion in several copper oxide compounds[22–26] and are pronounced enough to be observed in phonon density-of-states measurements as a softening of in-plane oxygen vibrational bands.[27,28] It is, therefore, quite justified to look at the phonon density-of-states of the nickelate as a function of hole concentration for signatures of electron-lattice coupling.

In the present experiment, the inelastic neutron-scattering spectra are measured for polycrystalline $La_{2-x}Sr_xNiO_4$ ($x=0$, 1/8, 1/4, 1/3, 1/2). The purpose is to obtain the dependence of the generalized (neutron scattering weighted) phonon densities of states (GDOS) on hole concentration, and also to determine the variation of the GDOS with temperature. Due to the likely interplay of the in-plane polarized

oxygen vibrations with hole localization and stripe order in the NiO_2 plane, the present study focuses on the in-plane oxygen vibrations. This is simplified due to the light mass of oxygen and the strong covalent Ni-O(1) bonds which separate the in-plane modes from others in the system. All phonon modes above 65 meV arise from in-plane polarized oxygen vibrations. This is the first systematic study of the doping and temperature dependence of the lattice dynamics of $La_{2-x}Sr_xNiO_4$ by neutron scattering.

$La_{2-x}Sr_xNiO_{4+\delta}$ polycrystalline samples were prepared by solid-state reaction of stoichiometric ratios of La_2O_3, $SrCO_3$, and NiO.[7] The $x=0$ and $x=1/8$ samples were subsequently annealed in flowing argon at 1100 °C for 20 h to ensure that $\delta \approx 0$.[4] X-ray powder-diffraction measurements at room temperature yielded lattice constant values consistent with previous reports[3] and indicated predominantly single phase material, with only a small x-independent La_2O_3 impurity phase. Magnetic-susceptibility measurements yielded data essentially equivalent to that of Cheong *et al.*,[7] including the reported signal of stripe order for $x=1/3$. Each sample weighed from 30 to 60 g.

Time-of-flight inelastic neutron-scattering measurements were performed on the Low Resolution Medium Energy Chopper Spectrometer (LRMECS) at Argonne National Laboratory's Intense Pulsed Neutron Source. Scattering angles (ϕ) from 2°–120° are covered by LRMECS. For all measurements, an incident neutron energy of 120 meV was chosen.

Powder samples were packed in flat-plate aluminum sample cans of dimensions $4'' \times 3'' \times 1/8''$ and oriented 45° to the incident beam direction. The sample can was mounted on a Displex closed-cycle He refrigerator for temperature dependence studies. Several samples were measured at 300 K in addition to the 10 K runs made for all samples. In addition, empty aluminum can and white beam vanadium runs were performed at room temperature for background and detector efficiency corrections, respectively. The data were also corrected for a time-independent intensity arising from the ambient neutron background, the k'/k phase space factor and sample self-shielding. To a first approximation, the experimental intensity $I(\phi,\omega)$ is proportional to the polycrystalline van Hove scattering function $S(\phi,\omega)$ plus a multiple-scattering contribution $M(\phi,\omega)$.

The reduced data $I(\phi,\omega)$ were summed over all scattering angles for each data set, giving a function $I(\omega)$. The GDOS can be obtained for each sample and temperature from the $I(\omega)$ data. However, we must first account for the multiple scattering mentioned previously and the multiphonon scattering. We expect inelastic magnetic contributions due to Ni spins to be present, but weak compared to the vibrational scattering in the angular range studied.

The multiple-scattering contribution was estimated from the data by extrapolating $I(\phi,\omega)$ to $\phi \rightarrow 0$ for several energy transfer ranges. The intensity at the $\phi=0$ intercept is assumed to arise from multiple scattering. The multiple-scattering contribution is also assumed to be independent of ϕ (as warranted by the small self-shielding corrections) and Sr concentration and is given by $M(\phi,\omega)=M(\omega)$.

In order to determine the multiphonon scattering, the nuclear neutron-scattering intensity of undoped La_2NiO_4 was calculated in the incoherent approximation. The partial phonon densities of states of La_2NiO_4 used in this calculation were obtained from a lattice-dynamical shell model for La_2CuO_4 after scaling the Cu/Ni mass. The use of the force constants of La_2CuO_4 is justified from the similarity of the phonon dispersion and density-of-states measurements for the undoped nickelate and cuprate compounds as demonstrated from the work of Pintschovius *et al.*,[21,28] as well as our own measurements.

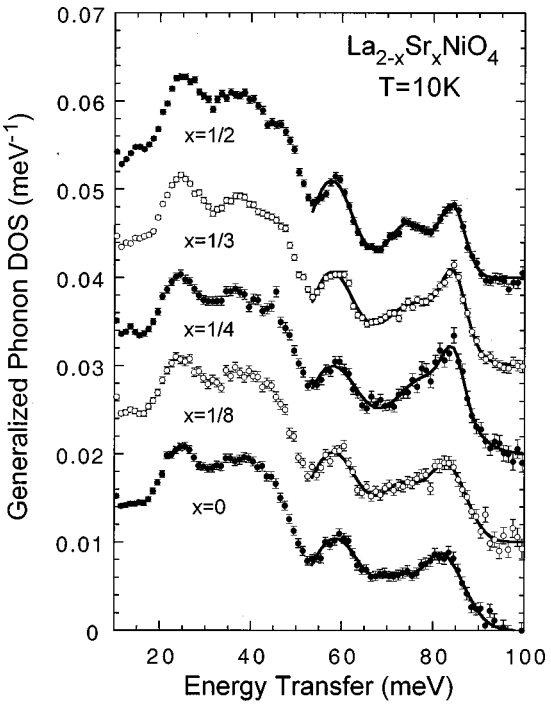

FIG. 1. Generalized phonon density-of-states of $La_{2-x}Si_xNiO_4$ for $x=0$, 1/8, 1/4, 1/3, and 1/2 at $T=10$ K. Solid line are Gaussian fits discussed in the text. Each data set is offset by 0.01 units.

From $I(\omega)$, we subtract the multiple and multiphonon scattering intensities and also subtract an elastic Gaussian which was obtained by fits to each data set. Due to the encroachment of the elastic peak and the large error associated with its subtraction, only the portion of the GDOS above 15 meV can be reliably obtained. The GDOS is then obtained by multiplying by $\omega/[n(\omega)+1]$, where $n(\omega)$ is the Bose population factor. Each GDOS was then normalized to one over the energy range from 15 to 100 meV.

The phonon GDOS is shown for $x=0$, 1/8, 1/4, 1/3, and 1/2 at 10 K in Fig. 1. The largest observed effect in the doping dependence is the gradual development of a subband at 75 meV from the main vibrational band at ~85 meV, particularly for $x=1/3$ and 1/2. In addition, there appears to be a narrowing of the ~60 and ~85 meV phonon bands and respective softening/hardening with hole doping. We also notice weak shifts towards higher frequencies for the 25 and 45 meV bands. The phonon bands above 50 meV were simultaneously fitted to three Gaussians and the phonon band positions and widths are plotted in Fig. 2. The fits are shown as solid lines in Fig. 1 and show the trends mentioned above with hole doping.

However, the Gaussian fits must be viewed with caution. We cannot know the precise functional form of the GDOS. We fit a Gaussian in the 65–80 meV range at low doping for which there is no discernible peak only to account for the tail

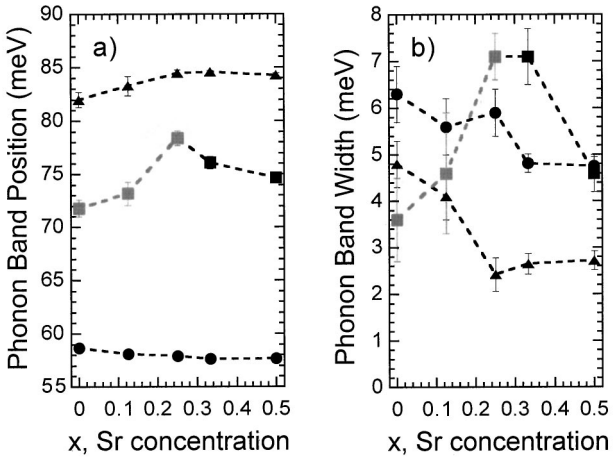

FIG. 2. Sr-doping dependence of (a) the phonon band position and (b) the phonon band width at $T=10$ K for bands at ~60 meV (circle), ~75 meV (square) and ~85 meV (triangle) as fit by a sum of three Gaussians. The shaded symbols correspond to a Gaussian contributing to the tail of the 85 meV peak and not to a well-defined peak, as discussed in the text.

of the GDOS below 85 meV (these are consequently grayed out in Fig. 2). Discretion must be used in the interpretation of the fits as the position and width parameters of the central and highest frequency Gaussians are correlated at low doping. In the case of $x=1/3$ and 1/2, there is a discernible peak and the central gaussian position has physical relevance.

Room-temperature measurements of several samples were also performed. The change in the GDOS at 300 K for $x=0$ consisted of the softening of some bands and an overall broadening of the features. In fact, the room-temperature results can be obtained from the 10 K results by broadening with a Lorentzian of width 2 meV. This is presumably due to normal anharmonic effects expected at high temperatures. The similarity of the 10 and 300 K runs for the cuprate sample $La_{1.9}Sr_{0.1}CuO_4$ (Ref. 29) indicates that the presence of the tetragonal-orthorhombic transition weakly affects, if at all, the frequency distribution of phonon modes. Rigid-ion lattice-dynamical models in both the tetragonal and orthorhombic phases of La_2NiO_4 support this conclusion.[30] The 300 K runs for $x=1/3$ and 1/2 have dependences which may be related to their respective charge ordering transition temperatures, however the association is only speculative and is not discussed here.[31]

Due to the weighting of the GDOS, the GDOS primarily consists of oxygen vibrations (~70%). For the undoped nickelate, two unique oxygen species exist; O(1), the planar oxygen, and O(2), the apical oxygen. From comparison to shell-model calculations, essentially all of the intensity above 50 meV is from oxygen, and as mentioned above, all the intensity above 65 meV arises from the in-plane polarized O(1) modes. The 85 meV vibrational band is comprised of Ni-O(1) bond-stretching modes, such as the oxygen breathing mode. From optical measurements[32,33] and shell-model results, the 60 meV band is associated with O(2) *c*-axis vibrations and in-plane Ni-O(1) bond-bending modes. Due to the inhomogeneous hole distribution, there may be several oxygen sites at larger doping which are chemically inequivalent.

Strontium doping should have several effects on the lattice dynamics. First, the substitution of strontium for lanthanum will increase the La/Sr vibrational frequency by about 25% due to the lighter mass of Sr. Since the maximum La phonon energy is ~25 meV, this effect is probably responsible for the small shift of the 25 meV peak to higher energies. The La(Sr)-O(2) vibrations would presumably soften due to the average reduction of valence at the La site. Also, Sr doping reduces the in-plane (*a*-axis) lattice constant and increases the out-of-plane (*c*-axis) lattice constant,[7] giving a concomitant hardening/softening for modes in the respective directions. Finally, we expect there to be some effect from the addition of holes into the NiO_2 plane from the electron-lattice coupling.

To date, only optical measurements have probed the dependence of the lattice dynamics of $La_{2-x}Sr_xNiO_4$ as a function of doping. Within the doping range studied here, the doping dependence of the modes probed by optical methods is simply explained by variations of the lattice constants and valence changes on the La site. On the contrary, it appears that the distinguishing features of the polycrystalline inelastic neutron-scattering data above 65 meV arise from a coupling to the holes themselves. This perhaps indicates that modes away from the zone center couple most strongly to the hole states. We see no difference between the undoped and $x=1/8$ sample. This is consistent with the optical results, since expected frequency shifts of the optical modes are less than ~0.5 meV at this concentration.[32,33]

Starting at low energies, the small shift of the 25 meV band is most likely a mass effect of Sr substitution. The movement of the 45 meV shoulder could arise from several kinds of Ni, O(1), and O(2) motions and cannot be ascertained. The respective softening/hardening of the 60/85 meV bands are likely related to the change in lattice constants with doping, as seen in the optical spectra. The narrowing of the 60 and 85 meV bands may be caused by the formation of local (flat optic) modes with hole density in the NiO_2 plane. At 10 K, the hole structures are periodic for $x=1/3$ and $x=1/2$, forming a stripe structure and a checkerboard pattern, respectively. In the presence of strong electron-lattice coupling, these structures may not allow many phonon modes to propagate, since the overwhelming majority are incommensurate with the charge structure. Thus, there is a tendency to flatten the optic branches of certain phonons.

The most interesting effect in the doping dependence is the creation of the 75 meV subband with increasing hole concentration. The subband at 75 meV most likely consists of oxygen bond-stretching vibrations at sites in the NiO_2 plane near to where holes reside. It has been proposed that oxygen breathing mode instabilities reinforce hole localization in these compounds.[15] The 75 meV subband may arise from the electron-lattice coupling of the breathinglike modes to the localized holes and presumably acts to stabilize polaron and stripe formations. Yi *et al.* have calculated the expected phonon spectrum in the presence of strong electron-lattice coupling and in the background of stripe order using an inhomogeneous Hartree-Fock method within the random-phase approximation. Yi *et al.* considered a small subset of possible atomic displacements, those being the longitudinal (bond-stretching) vibrations of the planar oxygens in a model of the NiO_2 plane. The theoretical results show the systematic evolution of a 75 meV band from the main 85 meV band

at $x=1/3$ and 1/2. While we cannot claim the uniqueness of Yi's model, the model suggests that the subband is associated with vibrational excitations of the stripe. Details of the comparison between these results and Yi's calculations will be discussed in an upcoming paper.[34]

For the $x=1/2$ checkerboard pattern, the sites with a localized hole appear to have a much softer spring constant, and vibrations taking place on either sublattice create two distinct phonon bands. Since the 75 meV subband formation is not a complete softening of main band for $x=1/2$, only certain types or certain symmetry phonons are affected. This implies that the electron-lattice coupling is only effectual for certain atomic displacements. Single-crystal phonon-dispersion measurements should contain large effects associated with hole doping for the oxygen optical branches.

As a last comment, it is interesting to compare this nickelate data to the lattice dynamics of the cuprates. Polycrystalline measurements of the phonon GDOS in the $La_{2-x}Sr_xCuO_4$ system indicate that the 80–90 meV in-plane oxygen phonon band softens quite significantly with relatively little doping ($x\approx 0.1$).[28] This softening is characterized by a transfer of GDOS weight from 90 meV to a subband at 75 meV for $x=0.1$ which continues to soften to 70 meV at $x=0.15$. Subsequent single-crystal measurements associate this softening with particular oxygen modes corresponding to Cu-O(1) bond-stretching vibrations along (1,0,0).[22] Such behavior has also been observed in many other copper-based superconductors, and appears to be a universal feature of the cuprates.[23,25–27] Using the present polycrystalline results as a comparison, subband formation for the in-plane oxygen modes in the nickelates has not yet occurred at $x=1/8$, but occurs somewhere between $x=1/8$ and 1/3. The rapid evolution of the insulator-metal transition with hole doping in the cuprates ($x\approx 0.05$), as opposed to the nickelates ($x\approx 1$), seems very relevant to the apparent difference in electron-lattice coupling in these compounds. Consequently, the electron-lattice coupling of certain modes in the cuprate may be strongly influenced by charge fluctuations.

We have measured the generalized phonon density of states as a function of doping for the charge-spin ordering system $La_{2-x}Sr_xNiO_4$ ($x=0$, 1/8, 1/4, 1/3, 1/2). We find no changes with temperature or doping for $x=0$ and 1/8. We do find evidence for unexpected renormalization of the planar oxygen phonon bands (60, 75, and 85 meV) which arise from a relatively high hole density in the NiO_2 plane. In particular, the in-plane bond-stretching band at 85 meV forms a softer subband at 75 meV which we ascribe to strong electron-lattice coupling. This coupling likely forms localized vibrations near doped holes which are related to polaron and/or stripe formation.

R.J.M. wishes to thank A. R. Bishop, Ya-Sha Yi, Tinka Gammel, T. Egami, and R. A. Robinson for stimulating discussions and S. Rosenkranz and E. Goremychkin for experimental assistance. This work was supported (in part) by the U.S. Department of Energy under Contract No. W-7405-ENG-36 with the University of California. This work has benefited from the use of the Intense Pulsed Neutron Source at Argonne National Laboratory. This facility is funded by the U.S. Department of Energy, BES-Materials Science, under Contract No. W-31-109-Eng-38.

[1] T. Ido *et al.*, Phys. Rev. B **44**, 12 094 (1991).
[2] S. Uchida *et al.*, Phys. Rev. B **43**, 7942 (1991).
[3] R. J. Cava *et al.*, Phys. Rev. B **43**, 1229 (1991).
[4] V. Sachan *et al.*, Phys. Rev. B **51**, 12 742 (1995).
[5] J. M. Tranquada, D. J. Buttrey, and V. Sachan, Phys. Rev. B **54**, 12 318 (1996).
[6] C. H. Chen, S.-W. Cheong, and A. S. Cooper, Phys. Rev. Lett. **71**, 2461 (1993).
[7] S.-W. Cheong *et al.*, Phys. Rev. B **49**, 7088 (1994).
[8] A. P. Ramirez *et al.*, Phys. Rev. Lett. **76**, 447 (1996).
[9] P. J. Brown *et al.*, Physica B **180-181**, 380 (1992).
[10] J. Zaanen and O. Gunnarsson, Phys. Rev. B **40**, 7391 (1989).
[11] V. J. Emery, S. A. Kivelson, and H. Q. Lin, Phys. Rev. Lett. **64**, 475 (1990).
[12] K. Yonemitsu, A. R. Bishop, and J. Lorenzana, Phys. Rev. B **47**, 12 059 (1993).
[13] J. Zaanen and P. B. Littlewood, Phys. Rev. B **50**, 7222 (1994).
[14] Y.-S. Yi *et al.*, Phys. Rev. B **58**, 503 (1997).
[15] V. I. Anisimov *et al.*, Phys. Rev. Lett. **68**, 345 (1992).
[16] P. Wochner *et al.*, Phys. Rev. B **57**, 1066 (1998).
[17] G. Blumberg, M. V. Klein, and S.-W. Cheong, Phys. Rev. Lett. **80**, 564 (1998).
[18] K. Yamamoto *et al.*, Phys. Rev. Lett. **80**, 1493 (1998).
[19] T. Katsufuji *et al.*, Phys. Rev. B **54**, R14 230 (1996).
[20] L. Pintschovius *et al.*, Europhys. Lett. **5**, 247 (1988).
[21] L. Pintschovius *et al.*, Phys. Rev. B **40**, 2229 (1989).
[22] L. Pintschovius *et al.*, Physica C **185-189**, 156 (1991).
[23] L. Pintschovius and M. Braden, J. Low Temp. Phys. **105**, 813 (1996).
[24] L. Pintschovius and W. Reichardt, in *Physical Properties of High Temperature Superconductors IV*, edited by D. Ginsberg (World Scientific, Singapore, 1994), p. 295.
[25] W. Reichardt *et al.*, Physica C **162-164**, 464 (1989).
[26] W. Reichardt, J. Low Temp. Phys. **105**, 807 (1996).
[27] R. Currat *et al.*, Phys. Rev. B **40**, 11 362 (1989).
[28] B. Renker *et al.*, Physica B **180&181**, 450 (1992).
[29] R. J. McQueeney (unpublished).
[30] N. Choudhury, K. R. Rao, and S. L. Chaplot, Physica C **171**, 567 (1990).
[31] R. J. McQueeney and J. L. Sarrao, in *High-Temperature Superconductivity and Related Topics*, edited by S. E. Barnes (AIP, University of Miami, in press).
[32] X.-X. Bi, P. C. Eklund, and J. M. Honig, Phys. Rev. B **48**, 3470 (1993).
[33] N. Ogita *et al.*, J. Phys. Soc. Jpn. **57**, 3932 (1988).
[34] Y.-S. Yi, R. J. McQueeney, and A. R. Bishop (unpublished).